

Improved Primary Reference Cell Calibrations for Higher Accuracy Photovoltaic Cell and Module Performance Measurements

Carl R. Osterwald, Larry Ottoson, Rafell Williams, Charles Mack, Jeremy Brewer, Nikos Kopidakis,* and Tao Song*

The adoption of photovoltaic (PV) modules for clean electricity relies on accurate measurements of their performance, which are essential for estimating their energy production potential. Herein, the calibration chain of PV cells and modules, with particular emphasis on primary reference cell calibrations, is discussed. Also, herein, the direct sunlight method the group has developed for these calibrations is presented and critical improvements and upgrades that lead to calibration uncertainty as low as 0.45% are discussed. The ultimate motivation behind this work is to provide low-uncertainty performance measurements of PV modules, and lowering the calibration uncertainty of primary reference cells is a key first step toward achieving this goal. As the use of solar electricity continues to grow, the demand for primary reference cell calibrations inevitably increases beyond what the small handful of primary calibration laboratories can provide today. Therefore, this work can serve as a useful guide for implementing primary PV reference cell calibrations using the outdoor method, as well as outlining the critical elements required to make these calibrations highly accurate.

1. Introduction

Solar photovoltaic (PV) cell and module researchers and manufacturers alike rely heavily on reference devices to accurately measure the performance of their products. On the one hand, these performance calibrations determine the power conversion efficiency at Standard Test Conditions (STC, detailed later), which is used to evaluate and compare cell and module technologies.^[1] On the other hand, the power rating of commercial PV modules, also measured at STC, is a key input factor in calculating the cost of solar electricity, usually presented either as cost per Watt of nominal power output by a PV module or as cost per KWh of energy produced by a complete PV system. Every measurement, including the PV performance measurements discussed in this article, is accompanied by an estimated


measurement uncertainty, and in the case of commercial PV modules, the uncertainty of the calibrated power of a module translates directly to an uncertainty of profit margin for the manufacturer.

Reducing the uncertainty of PV cell and module calibrations is a challenging task that starts with primary calibration laboratories striving to provide the PV community with highly accurate reference device calibrations, as we discuss later. As one of the few primary calibration laboratories worldwide, the PV cell and module performance team at the National Renewable Energy Laboratory (NREL) has dedicated years of effort to this task, resulting in a significantly reduced uncertainty of $\pm 0.8\%$ for the short-circuit current (I_{SC}) of silicon modules, down from $> \pm 3\%$ before implementing the improvements discussed here.^[2] As the I_{SC} from a refer-

ence module is used to set up the irradiance condition for module performance testing in a production line, low uncertainty calibration of a reference (“golden”) module translates directly to accurate power rating of production modules. For example, following the improvements we implemented, the expanded uncertainty for the maximum power (P_{MAX}) of silicon modules was decreased from $\pm 3.2\%$ to $\pm 1.1\%$.

The previously quoted uncertainties derive from a rigorous analysis^[2] based on the Guide to Uncertainty in Measurement,^[3] and have been approved under our group’s Scope of Accreditation to the ISO 17 025 quality control standard for PV reference module calibrations.^[4] The uncertainty of the reported performance parameters (I_{SC} , P_{MAX} , and the open-circuit voltage, V_{OC}) is calculated at the time of the measurement, since they also include module-specific contributions, and they represent the 95% confidence level for the reported value.^[3] Ultimately, the accuracy of the measurement including its uncertainty can only be verified by 1) analyzing repeat measurements on representative modules; and 2) intercomparisons with other accredited calibration laboratories. Since 2017, our group has conducted repeat measurements of a set of control modules of varying sizes. **Figure 1** depicts the I_{SC} history of one of these modules showing a standard deviation $2\sigma = 0.39\%$ (converted to relative change and multiplied by 2 for comparison to expanded uncertainty), well within the quoted expanded uncertainty of

C. R. Osterwald, L. Ottoson, R. Williams, C. Mack, J. Brewer, N. Kopidakis, T. Song
PV Cell and Module Performance Group
National Renewable Energy Laboratory (NREL)
15313 Denver West Parkway, Golden, CO 80401, USA
E-mail: nikos.kopidakis@nrel.gov; tao.song@nrel.gov

 The ORCID identification number(s) for the author(s) of this article can be found under <https://doi.org/10.1002/solr.202300379>.

DOI: 10.1002/solr.202300379

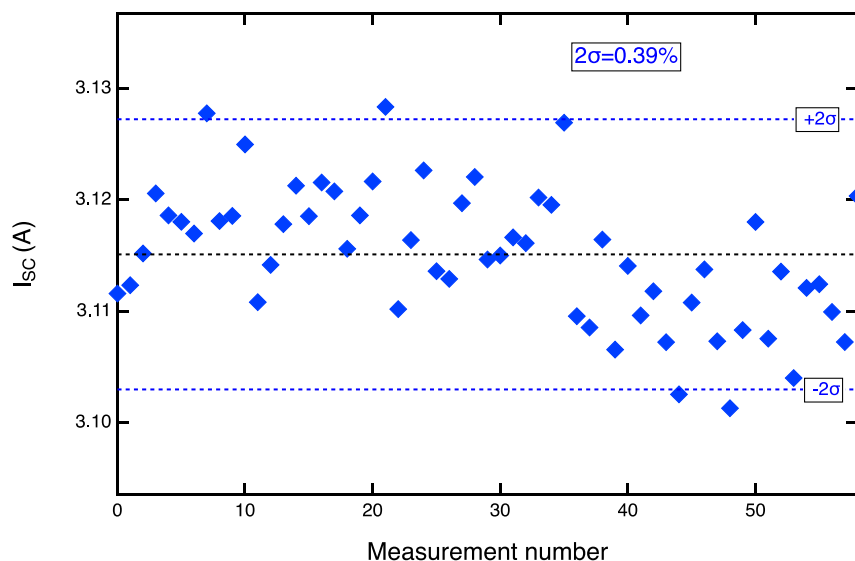


Figure 1. Repeat measurements of short-circuit current (I_{SC}) at standard test conditions (STC) for a 44.6 W silicon module. The measurements are carried out on average every 6 weeks, starting from 2017. The black dotted line shows the average I_{SC} and the blue dotted lines are $\pm 2\sigma$, where σ is the standard deviation of the data.

$\pm 0.8\%$ for I_{SC} . The observation of 2σ being comparable or lower than the estimated expanded uncertainty for I_{SC} , V_{OC} , and P_{MAX} holds for all control modules (not shown here), up to a module rated power of ≈ 350 W. Finally, the ultimate test of proficiency in performance measurements is intercomparison with other accredited calibration laboratories. The last published international module round robin, as reported in ref., [5] demonstrated excellent agreement between all participating laboratories. A more recent PV module intercomparison has also been completed with similar success and the results are yet to be published.

To achieve lower uncertainty in PV module calibrations, our group undertook two sequential steps. 1) Changes were implemented to hardware and data analysis to improve the accuracy of primary reference cell calibrations. The calibration of primary cells is transferred to all other calibrations of PV devices, including secondary reference cells and modules, and downstream PV products. Therefore, its accuracy is vital for accurate PV module calibrations. 2) Recognizing the limitations imposed by module-size solar simulators, we developed a module calibration method that takes advantage of the desirable aspects of three module testbeds to overcome limitations of performance measurements on individual testbeds. For example, the spatial nonuniformity of total irradiance of 2% in an indoor solar simulator (typical of a class A simulator) imposes a fundamental lower limit to the uncertainty of an I_{SC} measurement. By taking advantage of the highly uniform natural sunlight of our outdoor current-voltage (I - V) testbed, the I_{SC} measurement uncertainty can be further reduced to 0.8%.^[2]

In this article, we focus on step 1 and provide an overview of the different methods used by primary calibration laboratories worldwide. We then present the improvements that our group designed and implemented, providing key examples of how the changes to hardware and data analysis affected the primary

reference cell calibration results and quantifying the changes in calibration uncertainty. Finally, we verify the accuracy of our procedures by comparing them with other primary calibration laboratories internationally. With improved calibration methods for primary reference cells, we were able to proceed to step 2, which included the design and implementation of module-level measurement procedures, leading to low PV module calibration uncertainties as stated in our ISO accreditation and evidenced in the example of Figure 1. The discussion of these methods for PV modules will be presented in a later paper.

2. Primary Reference Solar Cell Calibration

The performance of PV cells and modules is dependent on various operational conditions, such as device temperature and spectral and total irradiance of the incident illumination. To enable accurate and standardized performance measurements of PV devices under different light sources and to facilitate meaningful comparison between various PV technologies, the PV community has developed a consensus of reporting performance at STC. For non-concentrator terrestrial PV devices, STC refers to a device temperature of 25 °C, under the global hemispherical reference spectral irradiance, known as AM 1.5 Global with a total irradiance of 1000 W m⁻² and a spectral irradiance distribution derived from a model of natural sunlight.^[6,7]

In practice, the performance of a PV device is usually measured using an indoor solar simulator, which unavoidably has a different spectral irradiance distribution than the reference spectrum. Hence, a spectral mismatch correction procedure in conjunction with calibrated reference cells is essential for accurate performance measurement of PV devices.^[8,9]

To set the desired simulator irradiance levels for the electrical performance measurement of PV devices, reference solar cells are used, and their calibration values (CVs) at STC should be

determined by qualified PV calibration laboratories and traceable to measurement standards and ultimately to the Système International (SI) units.^[10] **Figure 2** shows the most common calibration traceability chain for PV reference cells, which includes the irradiance calibration instruments in the PV community.^[11] The primary and secondary standards are associated with the instruments used for solar irradiance calibration, giving traceability to SI units. In the calibration chain, primary PV reference cells serve as the baseline for determining the lowest uncertainty of the measured performance of other PV reference devices including secondary reference cells and modules used by accredited testing labs^[1] and working reference cells typically used in research labs and industrial production. Multiple standardized routes for primary reference solar cell calibration are available, including the direct sunlight method used by NREL, indoor solar simulator method used by the National Institute of Advanced Industrial Science and Technology (AIST, Japan), and differential spectral responsivity (DSR) calibration used by the Physikalisch-Technische Bundesanstalt (PTB, Germany). Since the mid-1980s, NREL, as one of the few qualified primary calibration laboratories, has developed primary reference cell calibrations with a direct sunlight method. A detailed description of the other two methods can be found in IEC 60904-4.^[11]

2.1. NREL's Outdoor Primary Reference Cell Calibration Method

For NREL's primary reference cell calibration approach, the I_{SC} of the PV reference device under calibration is measured under

direct-beam natural sunlight as described later. Simultaneously with the reference cell I_{SC} measurement and reference cell temperature, the total irradiance (E_T) is measured with an absolute cavity radiometer (ACR) and the spectral irradiance ($E_{Meas}(\lambda)$) is measured with a spectroradiometer (SpR). All three types of devices, reference cell, ACR, and SpR, are fitted with collimating tubes to define a 5° field of view and mounted on 2-axis trackers programmed to continuously track the sun during the measurement window. Details of our calibration process have been published in refs. [12,13]

The CV of a reference cell illuminated by a given reference spectrum can be calculated using Equation (1) in $\text{mA (W/m}^2\text{)}^{-1}$

$$CV = \frac{I_{SC}}{E_T} \frac{1}{F} \quad (1)$$

where I_{SC} is the measured short-circuit current of the cell under direct sunlight, E_T is the total irradiance level measured with the ACR, and F is the spectral correction factor, expressed as

$$F = \frac{\int E_{meas}(\lambda) SR(\lambda, T_{meas}) d\lambda}{\int E_{meas}(\lambda) d\lambda} \times \frac{\int E_{ref}(\lambda) d\lambda}{\int E_{ref}(\lambda) SR(\lambda, T_{ref}) d\lambda} \quad (2)$$

where $E_{ref}(\lambda)$ is the reference spectral irradiance, and $SR(\lambda, T_{meas})$ and $SR(\lambda, T_{ref})$ are the spectral responsivity of the reference cell during the calibration and at reference temperature (25 °C), respectively. F is analogous but not identical to a spectral mismatch correction factor M . As we discuss in Section 2.2, an

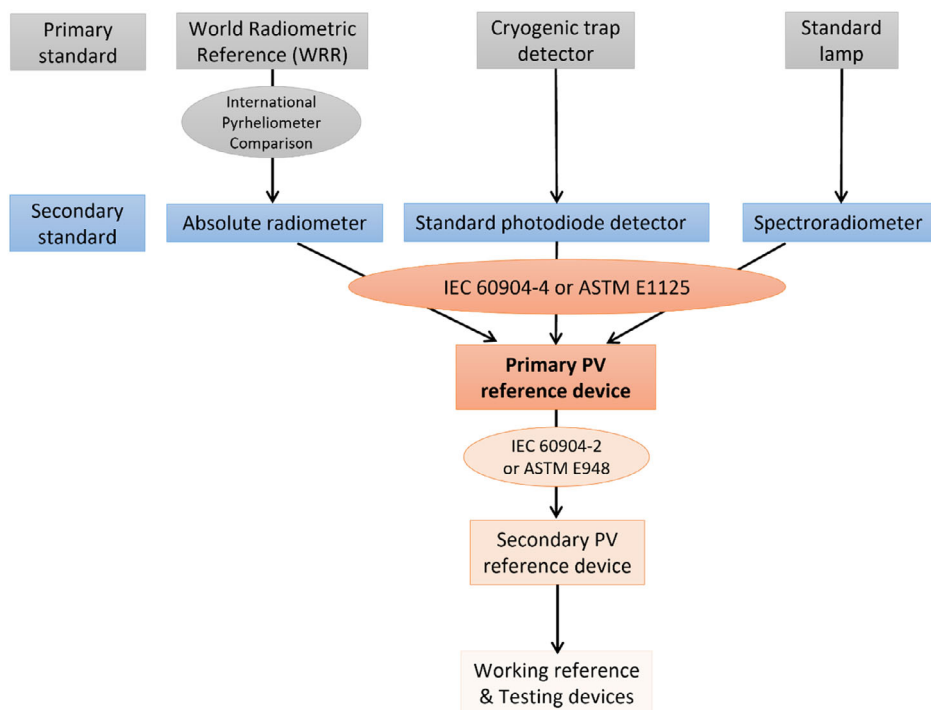


Figure 2. Traceable calibration chain of photovoltaic (PV) devices including the instruments for irradiance calibration, adapted from IEC 60904-4.^[11] Regarding different primary calibration routes, National Renewable Energy Laboratory (NREL)'s direct sunlight method involves the use of WRR-traceable absolute radiometers, Physikalisch-Technische Bundesanstalt (PTB)'s differential spectral responsivity (DSR) method used standard detectors, and the indoor simulator method adopted by AIST used absolute radiometers and standard lamps.

improved method for calculating Equation (2) is one of the key improvements in the primary calibration process.

For a world radiometric reference (WRR)-traceable calibration, as defined in Figure 2, the final primary CV is given by

$$CV_{WRR} = \frac{CV}{TF} \quad (3)$$

where CV arises from Equation (1) and TF denotes the transfer factor for converting the ACR measurement to the WRR standard. The WRR standard was established by the World Meteorological Organization (WMO) in 1977 and has been maintained by the Physikalisch-Meteorologisches Observatorium Davos-World Radiation Center (PMOD/WRC) in Switzerland. Every 5 years, the WRR is transferred to WMO regional centers and other participants including NREL's Solar Radiation Research Laboratory (SRRL) at the International Pyrheliometer Comparison (IPC) held at the PMOD/WRC.^[14] At each IPC, a new WRR-TF is calculated for each participating radiometer based on the mean WRR of the World Standard Group radiometers. Multiplying the irradiance reading of each radiometer by its assigned WRR-TF will result in measurements that are traceable to SI units through the WRR. The SRRL hosts annual NREL pyrheliometer comparisons (NPCs) for non-IPC years. NREL has developed the Transfer Standard Group (TSG) of four ACRs participated in the IPCs since 1990s to serve as the transfer reference for each NPC and thus to allow the transfer of the WRR to each participating radiometer. All subsequent ACRs in the annual NPC including the one used in our outdoor primary calibration is assigned a new WRR-TF, computed based on the NPC-TSG. A detailed description of this transferring process can be found at ref.[14] A history of the values of the TF is shown in Figure 3, indicating excellent stability of the ACR.

We note that the expanded uncertainty of the TF with respect to the SI unit, also provided after the annual pyrheliometer inter-comparisons, is $U(TF) = 0.39\%$ with a coverage factor $k = 2$ for the 2022 calibration (and similar in previous years) and cannot

currently be lowered by changes in hardware or data processing. The $U(TF)$ is a combined uncertainty from both the WRR scale with respect to SI unit and the ACR calibration in the NPC.^[14] Considering that $U(TF)$ is a fundamental lower limit to the uncertainty of a primary reference cell calibration in our WRR-traceable method, lowering the uncertainty of primary reference cell calibrations included improvements to the measurement of the cell's I_{SC} and to the calculation of F (Equation (2)), as described in Section 2.2. The ultimate verification that these improvements were successful is shown by intercomparison results with other primary calibration laboratories in Section 2.4.

2.2. Major Primary Calibration Improvements

Starting in 2014, a comprehensive effort was launched to improve NREL's primary calibration process, involving both software and hardware modifications.^[15] Figure 4 highlights the four major improvements that were made in comparison to the old process, including 1) upgraded spectral irradiance modeling and measurement to resolve spectral range discrepancy between reference and measured spectra; 2) a more rigorous temperature-dependent SR correction; 3) more accurate I_{SC} measurement with minimized stray light error; and 4) a visualized data-processing software for diagnosis and review purposes. In this subsequent section, we will give a detailed overview of the rationale and implementation of these improvements.

In the discussion of Equation (1) and (2) provided earlier, measurement of the spectral irradiance simultaneously with the I_{SC} of the cell is necessary for the calculation of the spectral correction factor, F . NREL had been using a portable LI-1800 SpR from LI-Cor Inc. for outdoor primary calibration since 1982. However, this SpR had a slow scan time of ≈ 30 s, and could only reliably detect wavelengths between 400 and 1000 nm using a Si photodiode detector. A major upgrade to improve primary calibrations was switching to a FieldSpec 3 SpR from ASD Inc., which has Si and InGaAs detectors and can collect 120 spectra during a 15 s

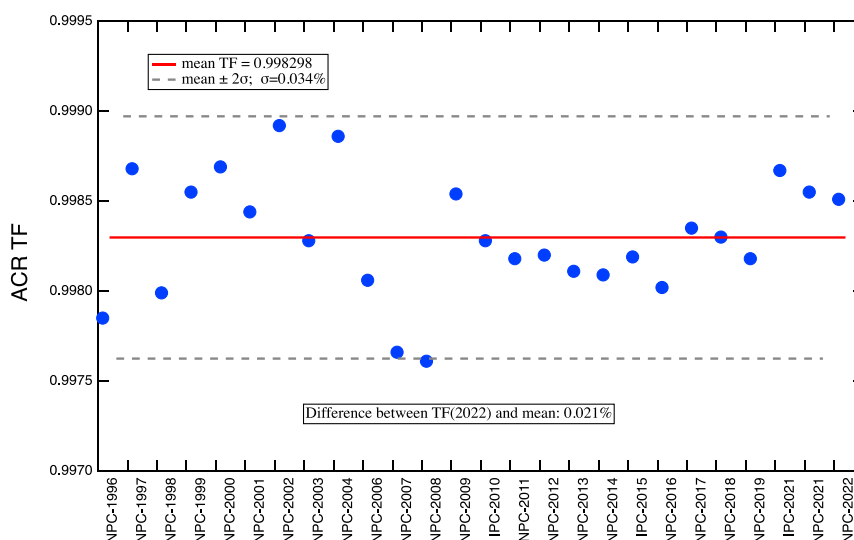


Figure 3. History of the numerical value of the transfer factor (TF) (see Equation (3)) for the absolute cavity radiometer (ACR) used for primary calibrations at NREL. NREL pyrheliometer comparison (NPC) denotes the annual National Pyrheliometer Comparison at NREL and IPC the International Pyrheliometer Comparison at the World Radiation Center in Davos, Switzerland.

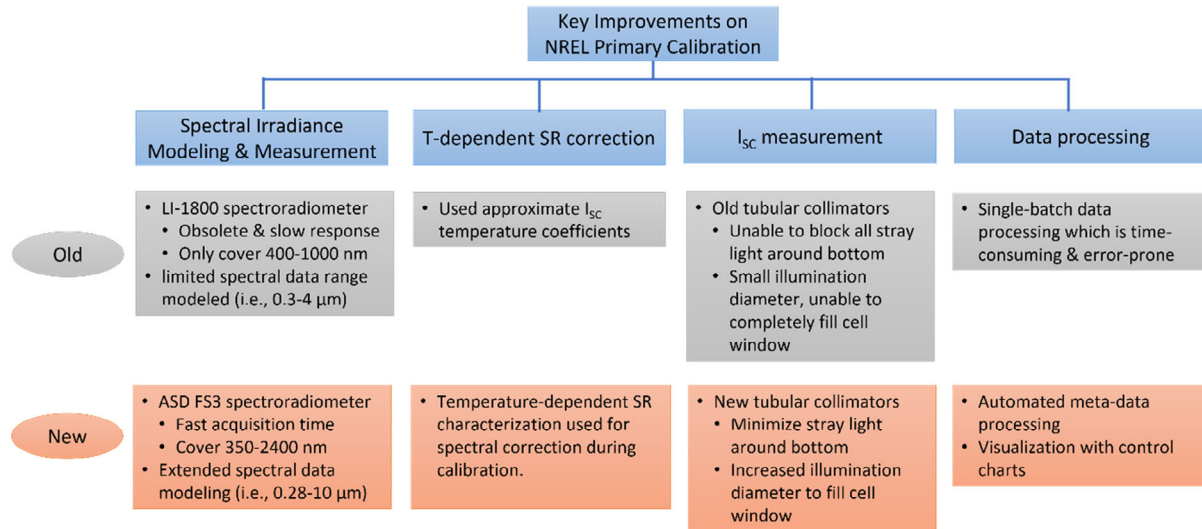


Figure 4. Key improvements on NREL outdoor primary calibration facility since 2014.

scan time in a wavelength range of 350–2400 nm. Note that the FieldSpec 3 SpR is calibrated annually at NREL's SRRL. The calibration follows the American Society of Testing and Materials (ASTM) standard, ASTM G-138-12: Standard Test Method for calibration of an SpR using a standard source of irradiance, and includes wavelength calibration, slit scattering test, spectral scattering test to check the stray light rejection and order sorting capabilities, and irradiance calibration with a national institutes of standards and technology (NIST) lamp. The spectral irradiance calibration uncertainties at the wavelengths from 350 to 2400 nm are less than $\pm 2\%$. The spectral irradiance acquisition during our primary calibration process is performed at the same SpR calibration temperature in the annual calibration. Since the I_{sc} and E_T are simultaneously sampled multiple times during the scan time, such a fast spectral irradiance acquisition time enables us to average any small irradiance changes during the measurement and thereby reduce spectral irradiance measurement errors. Additionally, we extended the wavelength range of our spectral irradiance modeling beyond 2400 nm, where the SpR cannot detect, for the F calculation. Note that the ACR used for measuring the total irradiance E_T of direct sunlight has a non-selective response in the infrared up until at least 10 μm . However, the global reference spectrum AM1.5G does not provide spectral irradiance data for wavelengths greater than 4 μm . As a result, the integral wavelength limits of the two definite integrals $\int_{\lambda_1}^{\lambda_2} E_{\text{meas}}(\lambda) d\lambda$ and $\int_{\lambda_1}^{\lambda_2} E_{\text{ref}}(\lambda) d\lambda$ in Equation (2) will be smaller and not represent the total irradiance measured by the ACR, leading to a measurement discrepancy in our CVs. To solve this wavelength limit discrepancy between ACR and reference spectrum, we implement a new spectral irradiance model that expands the measured spectral irradiance data from 2.4 out to 10 μm in the calculation of the spectral correction factor F . The spectral model also extends the lower limit of the spectral irradiance from 350 nm (the shortest detecting wavelength of FieldSpec 3 SpR) to 280 nm (the shortest wavelength of the tabulated AM1.5G spectrum). The extended spectral irradiance

data is calculated based on the atmospheric parameters in the AM1.5G spectrum^[6] and the MODTRAN code,^[16] and the total irradiance between 4 and 10 μm is estimated to be 2.9 W m^{-2} . With the new spectral irradiance extension modeling, we can fit our measured spectra to the ASD FieldSpec 3 SpR measurement to produce spectral irradiance over 0.28–10 μm , thus minimizing the calculation error of spectral correction factor caused by the wavelength limit discrepancy between ACRs and reference cells. The significance of these improvements is shown in Figure 5, where the influence of the limits of integration for Equation (2) is presented. The first and simplest choice would be to limit the integrals to the range where spectral irradiance data are obtained, i.e., from 350 nm to 2.4 μm . In this case, spectral modeling is not necessary since one can use the measured spectral irradiance from the SpR. Applying the spectral model as described earlier and detailed in ref.[17] allows one to extend the limits of integration since the modeled spectral irradiance during measurement extends beyond the SpR wavelength limits. Figure 5 shows example calculations of F using the spectral range of the published G173 spectrum (from 280 nm to 4 μm) and the extended G173 (from 280 nm to 10 μm). The results show that the choice of integration limits could change the applied correction by 0.5%, which is a substantial error (as we will show in the next section, a shift of the CV by 0.5% will cause significant discrepancies in intercomparison results with other primary calibration laboratories).

Another major improvement for our outdoor primary calibration is a more accurate I_{sc} measurement procedure for the reference cells. This involved redesigning the tubular collimators for mounting the reference cell and applying a more rigorous temperature coefficient correction during the calibration. Our reference cell tracker can simultaneously measure the I_{sc} of four cells using four collimators. The old design of the collimators could not prevent all stray light around the bottom from reaching the reference cells, and the 40 mm diameter illumination area did not completely fill the glass windows of some packaged reference cells with large window sizes. To address these issues,

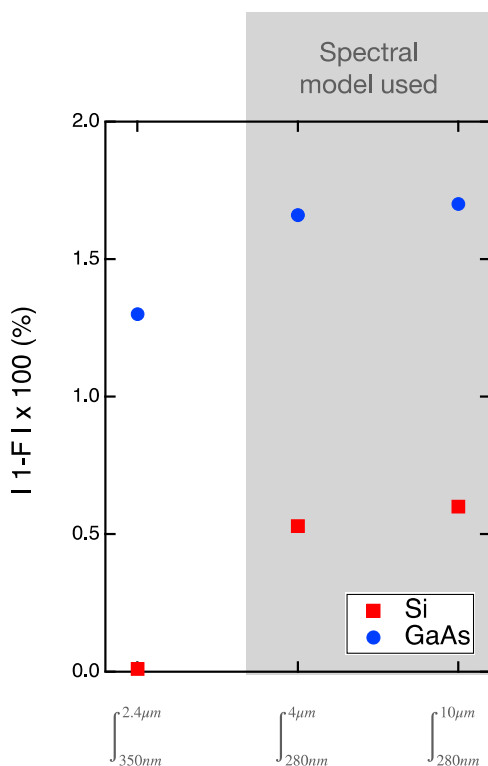


Figure 5. Spectral correction, calculated as percent deviation from unity, for two representative reference cells, Si (red) and GaAs (blue), as a function of the limits of integration in Equation (2). The gray highlight shows where spectral modeling must be applied to the measured spectral irradiance to allow extending beyond the 350 nm–2.4 μ m measured data.

we increased the diameter of the collimators to 80 mm and redesigned their inner aperture locations to minimize off-angle illumination from reflections. We also increased the distance between the last inner aperture and the reference cell top surface and sealed a gasket around the collimator bottom edges to minimize the stray light effect. The mounting plate for the reference cells in the tracker is temperature controlled and can accommodate four cells. Due to variations of the dimensions and construction of the package between cells, a temperature variation of ± 2 from 25 $^{\circ}$ C is possible during the scan, introducing I_{SC} measurement errors. In the past, we used empirical I_{SC} temperature coefficients measured with temperature-dependent I – V (I – V – T) to correct this error. However, these coefficients are only approximation of the I_{SC} variation with temperature and are in principle functions of spectral irradiance. To develop a more rigorous I_{SC} correction, we calculated the temperature-dependent SR by measuring SR at different temperatures from 15 to 40 $^{\circ}$ C. Then, we implemented this quantitative $\partial SR/\partial T$ profile into Equation (2) for the temperature correction. A detailed deduction of this correction can be found at refs. [15,18]

The last major improvement to our primary calibration process is the development of the new automated data process software. During each year's primary calibration cycle, there are >3600 data files generated for our 30–40 reference cells, and the post-processing of these files for spectral- and temperature-corrected CVs was previously done as a single batch

operation. Diagnosing bad data points was a time-consuming and non-user-friendly process. A new data-processing LabVIEW software has been developed to automate the process. It enables visualization of an individual reference cell in the entire annual calibration cycle such as I_{SC} , E_T , and wind speed, using a control chart of CVs that include all the measurement data points, making it easy to visually identify any abnormal device behaviors or bad points that fail to meet the requirements of primary testing conditions. The software also makes it easy for the data reviewer to analyze the primary calibration dataset including all past calibration history for a given cell thereby making it easy to flag unstable or degrading cells.

2.3. Uncertainty Budget

After implementing the aforementioned improvements, the expanded measurement uncertainty $U_{K=2}$ (CV) of our primary CVs has been reduced from approximately 1.0% to $\approx 0.45\%$ for typical Si reference cells. **Table 1** compares the estimated main standard uncertainty components in NREL's primary calibration before and after the improvements. The standard uncertainty of the total irradiance E_T measurement, $u(E_T)$, is from the ACR, which has participated in annual NPC for over 27 years, and has an estimated expanded uncertainty of 0.38% ($k = 1.96$) with respect to the SI unit in 2022.^[14] Therefore, the standard uncertainty of E_T is calculated as $u(E_T) = 0.38\%/1.96 = 0.194\%$. In terms of the uncertainty of spectral correction factor, $u(F)$, we previously adopted a fixed conservative $u(F)$ estimate of 20% of spectral correction factor variation due to the large measurement uncertainty of the old spectral irradiance measurement. For instance, the spectral correction factor is typically unity within 2% (i.e., 0.98–1.02) and accordingly the estimated standard uncertainty $u(F)$ is $0.4\% = 2\% \times 20\%$, as shown in Table 1. A Monte Carlo simulation study^[19] suggests that $u(F)$ is proportional to the magnitude of the correction from unity, and estimating $u(F)$ based on a Monte Carlo simulation necessitates identifying the spectral regions that contribute to uncertainty.^[20] However, using this proportionality, assumption to the magnitude of F is not a practical way to accurately account for $u(F)$ because the proportionality constant is unknown for each

Table 1. Estimated key standard uncertainty components for the calibration values of a world photovoltaic scale (WPVS) packaged Si reference cell measured with NREL's outdoor primary calibration process: old versus improved facilities.

Uncertainty components	Value of uncertainty [%]	
	Old facility	Improved facility
Total direct irradiance E_T measured with ACR, $u(E_T)$	0.189	0.194
Uncertainty of spectral correction factor F , $u(F)$	0.4	0.095
I_{SC} measurement with digital voltage meter (DVM) (temperature correction included), $u(I_{SC})$	0.169	0.033
Combined standard uncertainty of the calibration value	0.474	0.219

calibration point. Instead, the $u(F)$ is estimated by the standard deviation of the repeated measurements of the CVs of each reference cell in the entire calibration process, which lasts for multiple weeks under varying spectral and total irradiance conditions. Note that our outdoor primary calibration is performed in mornings with clear-sky direct solar irradiance and the air mass is less than 3.0 with a total irradiance in the 750 and 1100 W m⁻² range, which naturally also involves a measurement of I_{SC} linearity versus irradiance. All our primary reference cells are scrutinized for this dependence and shown excellent linearity in I_{SC} in the 750–1100 W m⁻² irradiance range. If nonlinear behavior is observed, extra measurement uncertainty from non-linearity should be considered. Typically, ≈ 100 measurements of the CV, denoted later as CV_i , $i = 1–100$, of each cell, according to Equation (3), are taken for every calibration cycle and averaged to produce the final reported CV. As we discuss later, lower standard deviation (σ) of the measured values will lead to lower standard deviation of the final CV and the top panels of **Figure 6** demonstrate the importance of the spectral correction for reducing σ : for the raw CV measurements prior to spectral correction, $\sigma = 1.4\%$, while after spectral correction as described in detail earlier, $\sigma = 0.09\%$. Figure 6a also shows that the raw measured values are not normally distributed, but a rather steplike behavior is observed where each individual step corresponds to a daily dataset and a distinctly different spectral irradiance shape for that day. For this reason, the standard deviation of the averaged CV of a cell during a calibration cycle is not estimated as the standard

error of the mean, $\frac{\sigma}{\sqrt{N}}$, where σ is the standard deviation of the measured values and N is the number of points averaged. Since the measurement conditions vary, the uncertainty of the final CV includes the standard deviation of the measurement points according to the weighted variance method. The weighted variance of the average CV is given by

$$\sigma^2(CV) = \frac{1}{m} \sum_{i=1}^m [CV_i^2 + \sigma^2(CV_i)] \quad (4)$$

where m is the number of CVs measured, CV_i denotes individual CV measurement, and $\sigma^2(CV_i)$ is its variance in absolute units. The final combined uncertainty of the average CV in relative percent is then given by

$$u(CV) = 100 \frac{\sqrt{\sigma^2(CV) - (CV)^2}}{CV} \quad (5)$$

As described earlier, this includes the standard deviation of the measured CVs and is a good representation of the uncertainty of the final averaged value given the variation in measurement conditions. An illustrative example is shown in Figure 6. In this case, the estimated uncertainty of each measurement is 0.55% and the standard deviation between points is 0.095%. Using the weighted variance method to combine uncertainties, the expanded uncertainty of the average CV is 0.58%.

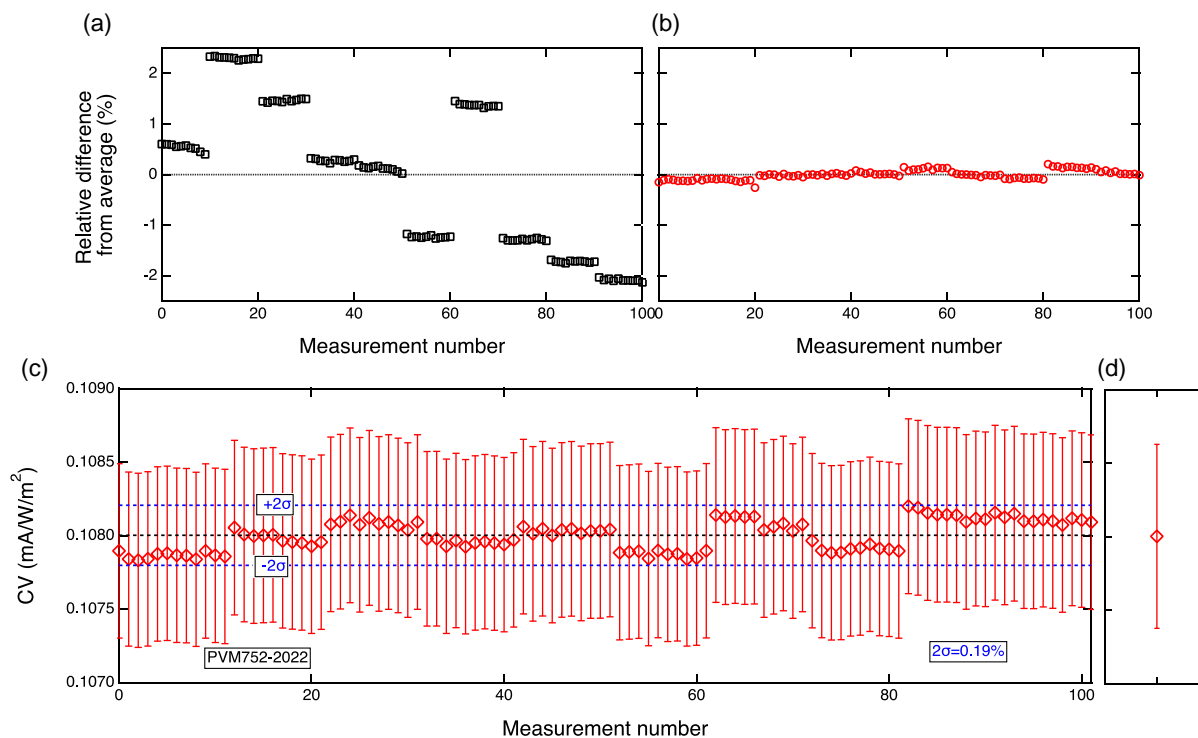


Figure 6. Top panels: calibration values (CVs) of a GaAs reference cell during the 2022 primary calibration cycle shown as relative deviation from the average: a) prior to spectral correction and b) after spectral correction according to Equation (1) and (2). Bottom panels: c) corrected CV including measurement uncertainty. The black dotted line shows the average value and the blue dotted lines correspond to $\pm 2\sigma$, where σ is the standard deviation of the measured values. d) The final CV from the 2022 calibration cycle for this cell, taken as the average of all points, and its associated expanded uncertainty of 0.58%.

It is evident from the example of Figure 6 that low standard deviation between measurements within a calibration cycle is crucial for achieving a low uncertainty for the resulting CV. After the improved primary calibration process, the standard deviation of all the measurement points for our reference cells has been significantly reduced, as shown in two representative examples in Figure 7. With more reliable spectral irradiance modeling and measurement, the spectral correction can be more accurately performed on the measured data points spanning several days. Therefore, the improvements described earlier decreased 2σ from 0.42% to 0.19% and from 0.60% to 0.18% for two representative GaAs reference cells.^[21]

Additionally, the measurement consistency between years has also been significantly improved since 2016. Figure 8 shows the statistical control chart of the averaged daily CV for mono-Si reference cell 002–215, one of our primary reference cells calibrated from 2016 to 2022. The overall standard deviation of the 68 day CVs in the past 7 years is 0.13% relative to the mean CV, which is much tighter than the CVs calibrated with the old facility before 2016 (i.e., ≈ 0.5 – 0.7% and examples shown in Figure 7), and furthermore all the data points fall into the $\pm 2\sigma$ limits. The other NREL primary reference cells also show the same improved calibration consistency after the facility upgrade.

The previous discussion highlights the importance of tight control of the measurement conditions to produce a small standard deviation between the ≈ 100 measurements of the CV taken

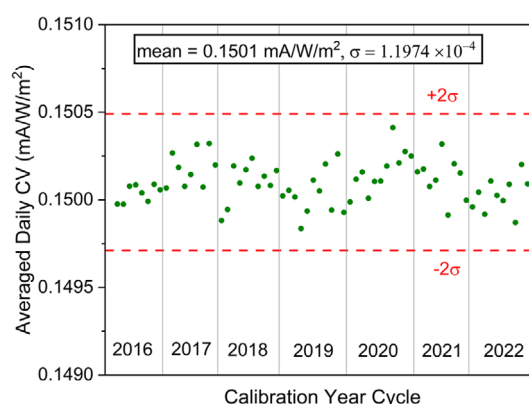


Figure 8. Control chart of daily averaged CVs of mono-Si reference cell 002–215 from 2016 to 2022. In this chart, the CV points shown are the average of ≈ 10 individual measurements each day. The standard deviation of the CVs is $1.1974 \times 10^{-4} \text{ mA (W}^{-1} \text{m}^{-2})$ or 0.132% relative to the mean CV in 2016–2022.

for each cell during a calibration cycle. Also important is a low uncertainty for each of these measurements, as discussed in the following. Overall, the standard uncertainty of I_{SC} measurement has also been reduced from 0.17% to 0.033% with an improved temperature correction procedure described in Section 2.2. In

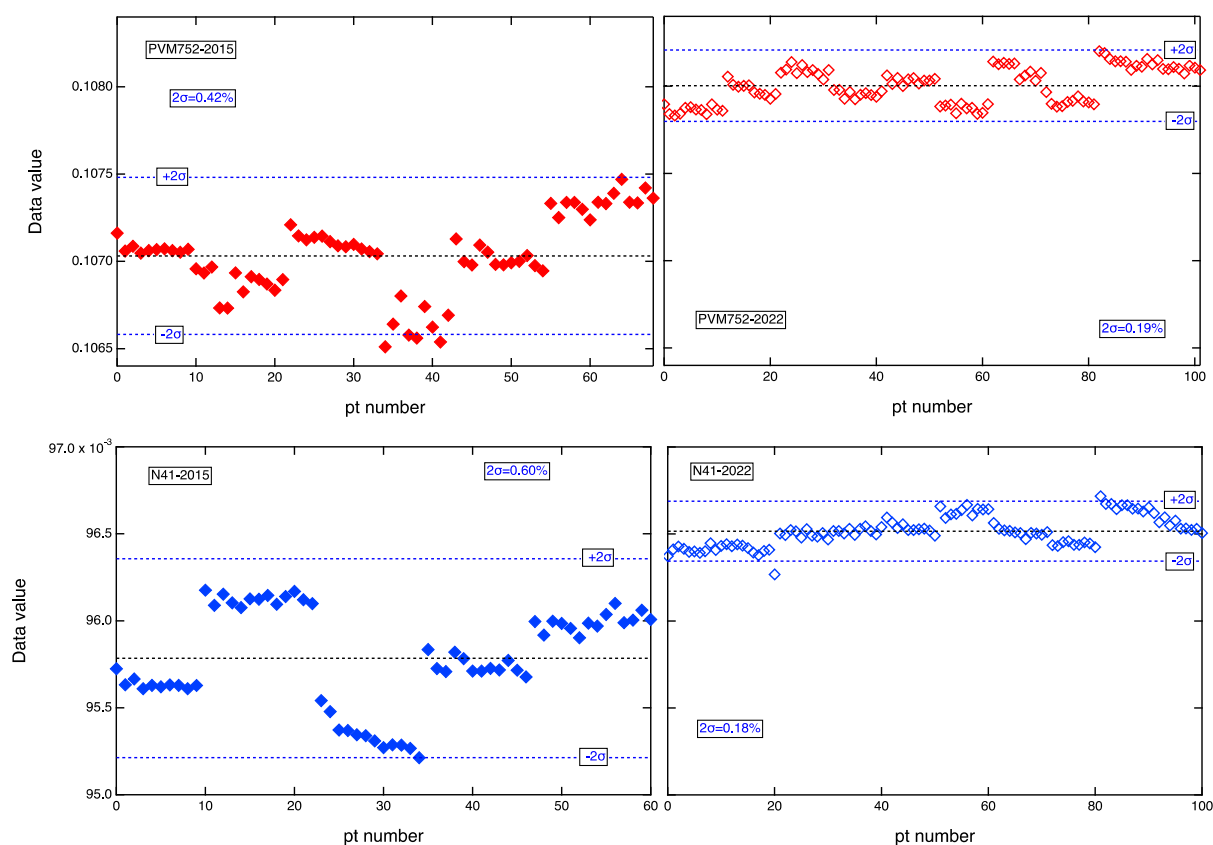


Figure 7. Calibration data for two GaAs reference cells, PVM752 and N41. Solid symbols: 2015 calibration cycle, prior to implementation of the improvements described here. Open symbols: calibration data for the 2022 calibration cycle.

summary, the combined uncertainty of individual measurements of the CV for a typical Si primary reference cell at NREL is now estimated as

$$u(CV_i) = \sqrt{u(E_T)^2 + u(F)^2 + u(I_{SC})^2} \quad (6)$$

$$= \sqrt{0.194^2 + 0.095^2 + 0.033^2} = 0.219\%$$

compared to 0.47% in the old primary calibration process. Using a coverage factor $k=2$, the expanded measurement uncertainty of the CV for this cell is reduced from $\pm 0.95\%$ to $\pm 0.44\%$. As mentioned earlier, an extra nonlinearity measurement uncertainty component should be included if a reference cell is observed with nonlinear I_{SC} versus total irradiance values.

2.4. Intercomparison Results

To validate the effectiveness of our improved primary calibration process, we have conducted multiple rounds of intercomparison with other qualified primary calibration laboratories such as PTB in Germany and AIST in Japan in the past few years. In 2016, after completing all upgrades, we compared the primary calibration results of six primary Si reference cells between NREL and PTB. As shown in Figure 2, PTB uses the DSR method to conduct the primary calibration, and the CV is derived from the measured absolute SR of the reference PV devices and the reference spectrum.^[22] In contrast, NREL's direct sunlight method measures the total solar irradiance with an ACR, calibrated and traceable to WRR, and does not require absolute SR calibration. Instead, the calculation of spectral correction

factor shown in Equation (2) only needs a relative SR profile. The intercomparison results of the six Si primary reference cells between NREL and PTB, conducted using two totally different methods, are shown in Figure 9a. The CVs of the six Si reference cells between the two primary calibration methods are in excellent agreement within the measurement uncertainties quoted by both laboratories, which validates the effectiveness of our improved primary calibration process.

In 2022, we conducted another round of intercomparison to check the calibration robustness on reference cells covering different spectral response ranges. Three different types of Si primary reference cells from PTB were compared, as shown in the quantum efficiency profiles of Figure 9b, with two of them being UV and IR filtered, respectively. The KG-filtered Si reference cell is normally used for the performance calibration of wide bandgap solar cells such as the currently popular perovskite material, and the UV-filtered Si reference cell is used for the spectral irradiance adjustment of bottom junctions in perovskite-related two-junction cells (e.g., all-perovskite tandem, perovskite/Si). Figure 9c shows the comparison results of the three different types of primary reference cells between our two laboratories. Note that the larger uncertainty bars of the KG-filtered and UV-filtered Si cells at NREL are due to an estimated larger spectral correction factor error.^[23]

As mentioned in Section 2.2, a 0.5% systematic error in the CV could arise from the narrower choice of integration limits for F in the absence of a spectral model. The intercomparison results presented in Figure 9 show that such a systematic error will negate the observed agreement of our results and those of other WPVS laboratories. This further demonstrates the importance of

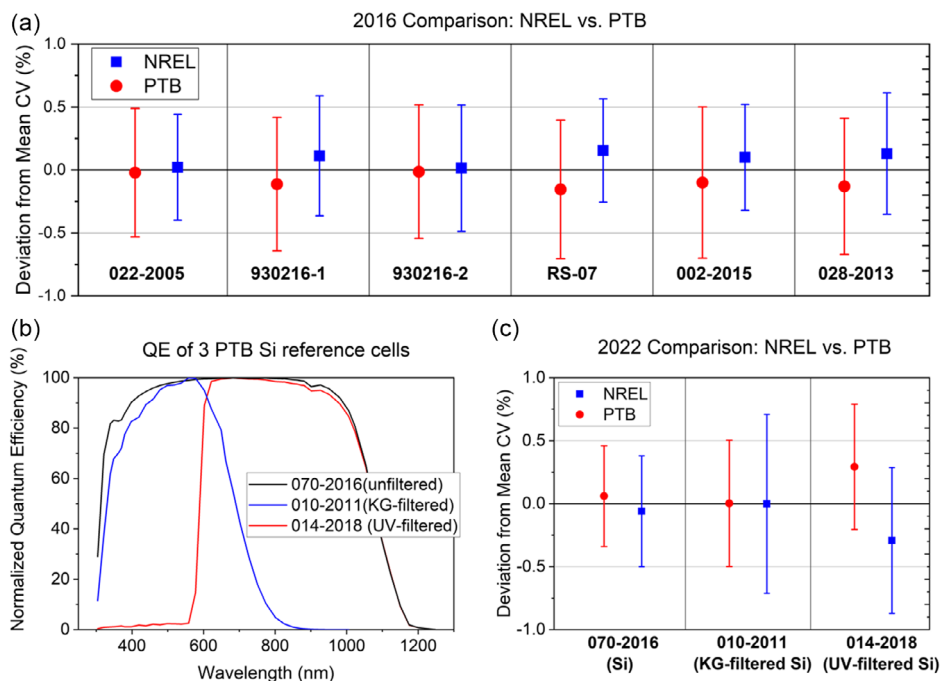


Figure 9. a) Primary CV comparison of six mono-Si primary reference cells (unfiltered and filtered) calibrated by NREL and PTB in 2016; b) normalized quantum efficiencies of three different types of Si primary reference cells used in 2022 comparison; and c) CV comparison of the three cells calibrated by NREL and PTB in 2022.

spectral modeling as implemented in our primary calibration data processing.

3. Summary and Conclusions

Overall, the improved primary calibration process at NREL has enabled us to provide one of the lowest uncertainties for primary PV reference cell calibration worldwide. This is crucial because, as illustrated in the calibration chain of Figure 1, all the secondary PV cell and module testing relies on the accuracy of primary calibration results. This advancement ensures that we deliver highly accurate performance calibration on secondary PV reference devices, as well as PV cells and modules from researchers and manufacturers. This achievement is particularly important in light of the enormous global PV market, which exceeded 1 Terawatt (TW) of installed capability worldwide in 2022 and is projected to reach 75 TW by 2050 to address greenhouse gas emissions while meeting global energy need for the future.^[24] The improvement in measurement accuracy of primary reference cell calibrations will benefit the global PV industry, as a 1% reduction in measurement uncertainty in the commercial module performance calibration chain could result in a more accurate module power gauge of 0.75 TW in a 75 TW scale PV market, with a far-reaching impact on all energy stakeholders. As briefly mentioned in the introduction, by leveraging the advancement of our primary cell calibration accuracy and the improved module measurement protocol, NREL has significantly reduced the measurement uncertainty for secondary module performance calibration in commercial Si modules from $\pm 3.2\%$ to $\pm 0.7\%$ for I_{SC} and from $\pm 3.3\%$ to $\pm 1.1\%$ for P_{MAX} . A detailed discussion on this module performance calibration improvement will be presented in a follow-up paper.

Acknowledgements

The authors would like to thank their retired colleague Keith Emery who supervised the initial primary calibration improvements. The authors would also like to thank Ingo Kröger and Stefan Winter of PTB for providing intercomparison reference cell calibrations in the past years. This work was authored by Alliance for Sustainable Energy, LLC, the manager and operator of the National Renewable Energy Laboratory for the U.S. Department of Energy (DOE) under Contract No. DE-AC36-08GO28308. Funding was provided by U.S. Department of Energy Office of Energy Efficiency and Renewable Energy Solar Energy Technologies Office (SETO) Agreement No. 38262. The views expressed in the article do not necessarily represent the views of the DOE or the U.S. Government.

Conflict of Interest

The authors declare no conflict of interest.

Data Availability Statement

The data that support the findings of this study are available from the corresponding author upon reasonable request.

Keywords

absolute cavity radiometer, measurement uncertainty, primary reference cell calibration, PV modules, solar cells, spectroradiometer

Received: May 18, 2023

Revised: June 29, 2023

Published online: August 11, 2023

- [1] M. A. Green, E. D. Dunlop, G. Siefer, M. Yoshita, N. Kopidakis, K. Bothe, X. Hao, *Prog. Photovoltaics Res. Appl.* **2023**, 31, 3.
- [2] D. H. Levi, C. R. Osterwald, S. Rummel, L. Ottoson, A. Anderberg, in *2017 IEEE 44th Photovoltaic Specialist Conference (PVSC)*, IEEE, Piscataway, NJ pp. 467–471, **2017**.
- [3] Bureau International des Poids et Mesures, Joint Committee for Guides in Metrology, JCGM 100 **2008**, <http://www.bipm.org> (accessed: May 2023).
- [4] NREL Photovoltaic Device Performance Calibration Services, <https://www.nrel.gov/pv/pvdp/about.html> (accessed: July 2023).
- [5] E. Salis, D. Pavanello, M. Field, U. Kräling, F. Neuberger, K. Kiefer, C. Osterwald, S. Rummel, D. Levi, Y. Hishikawa, K. Yamagoe, H. Ohshima, M. Yoshita, H. Mülleijans, *Sol. Energy* **2017**, 155, 1451.
- [6] ASTM G173-03, *Standard Tables for Reference Solar Spectral Irradiances: Direct Normal and Hemispherical on 37° Tilted Surface*, ASTM, Philadelphia, PA **2006**.
- [7] IEC 60904-3, *Photovoltaic Devices – Part 3: Measurement Principles for Terrestrial Photovoltaic (PV) Solar Devices with Reference Spectral Irradiance Data*, Geneva, Switzerland **2019**.
- [8] ASTM E973-16, *Standard Test Method for Determination of the Spectral Mismatch Parameter Between a Photovoltaic Device and a Photovoltaic Reference Cell*, Philadelphia, PA **2020**.
- [9] IEC 60904-7, *Photovoltaic Devices – Part 7: Computation of the Spectral Mismatch Correction for Measurements of Photovoltaic Devices*, Geneva, Switzerland **2019**.
- [10] C. R. Osterwald, S. Anevsky, K. Bücher, A. K. Barua, P. Chaudhuri, J. Dubard, K. Emery, B. Hansen, D. King, J. Metzendorf, F. Nagamine, R. Shimokawa, Y. X. Wang, T. Wittchen, W. Zaaïman, A. Zastrow, J. Zhang, *Prog. Photovoltaics Res. Appl.* **1999**, 7, 287.
- [11] IEC 60904-4, *Photovoltaic Devices – Part 4: Photovoltaic Reference Devices – Procedures for Establishing Calibration Traceability*, Geneva, Switzerland **2019**.
- [12] C. R. Osterwald, K. A. Emery, D. R. Myers, R. E. Hart, in *21st Photovoltaic Specialists Conf.* **1990**.
- [13] K. A. Emery, C. R. Osterwald, *Sol. Cells* **1986**, 17, 253.
- [14] I. Reda, A. Andreas, M. Stoddard, M. Kutchenreiter, A. Habte. NREL Pyrheliometer Comparisons: September 25 – October 1, 2022 (NPC2022), <https://aim.nrel.gov/npc.html#NPC2022>.
- [15] C. R. Osterwald, L. Ottoson, R. Williams, C. Mack, T. Moriarty, K. A. Emery, D. H. Levi, in *2017 IEEE 44th Photovoltaic Specialist Conf. (PVSC)*, IEEE, Piscataway, NJ **2017**, pp. 490–495.
- [16] ASTM E1125-16, *Standard Test Method for Calibration of Primary Non-Concentrator Terrestrial Photovoltaic Reference Cells Using a Tabular Spectrum* **2016**.
- [17] C. R. Osterwald, K. A. Emery, *J. Atmos. Oceanic Technol.* **2000**, 17, 1171.
- [18] C. R. Osterwald, M. Campanelli, T. Moriarty, K. A. Emery, R. Williams, *IEEE J. Photovoltaics* **2015**, 5, 1692.
- [19] H. Field, K. Emery, in *23rd IEEE Photovoltaic Specialists Conf.*, IEEE, Piscataway, NJ **1993**, pp. 1180–1187.
- [20] J. Hohl-Ebinger, W. Warta, *Prog. Photovoltaics* **2011**, 19, 573.

- [21] C. Osterwald, *NREL Uncertainty of Photovoltaic Primary Reference Cell Calibration*, <https://www.nrel.gov/pv/pvdp/publications.html> (accessed: 2018).
- [22] S. Winter, T. Fey, I. Kröger, D. Friedrich, K. Ladner, B. Ortel, S. Pendsa, F. Witt, *Measurement* **2014**, 51, 457.
- [23] T. Song, R. Williams, L. Ottoson, C. Mack, J. Geisz, J. Brewer, N. Kopidakis, *IEEE J. Photovoltaics*, accepted.
- [24] N. M. Haegel, P. Verlinden, M. Victoria, P. Altermatt, H. Atwater, T. Barnes, C. Breyer, C. Case, S. De Wolf, C. Deline, M. Dharmrin, B. Dimmler, M. Gloeckler, J. C. Goldschmidt, B. Hallam, S. Haussener, B. Holder, U. Jaeger, A. Jaeger-Waldau, I. Kaizuka, H. Kikusato, B. Kroposki, S. Kurtz, K. Matsubara, S. Nowak, K. Ogimoto, C. Peter, I. M. Peters, S. Philipps, M. Powalla, et al., *Science* **2023**, 380, 39.